Numerical modeling of an impact-induced hydrothermal system at the Sudbury crater

Oleg Abramov and David A. Kring
Lunar and Planetary Laboratory, University of Arizona, Tucson, Arizona, USA

Received 11 November 2003; revised 11 May 2004; accepted 17 June 2004; published 20 October 2004.

[1] Large impact events, like the one that formed the Sudbury crater in Ontario, Canada, at 1.85 Ga, significantly increase the temperature of target rocks. The heat sources generated by such an impact event can drive the circulation of groundwater, establishing a hydrothermal system. We report on the results of numerical modeling of postimpact cooling with and without the presence of water at the Sudbury crater. A hydrothermal system is initiated in the annular trough between the peak ring and final crater rim, perhaps venting through faults that bound blocks of the crust in the modification zone of the crater. Although circulation through the overlying breccias may occur in the center of the crater, the central melt sheet is initially impermeable to circulating fluids. By $\sim 10^5$ years the central melt sheet crystallizes and partially cools, allowing fluids to flow through it. Host rock permeability is the main factor affecting fluid circulation and lifetimes of hydrothermal systems. High permeabilities lead to a rapid system cooling, while lower permeabilities allow a steady transport of hot fluids to the surface, resulting in high surface temperatures for longer periods of time than cooling by conduction alone. The simulations presented in this paper show that a hydrothermal system at a Sudbury-sized impact crater can remain active for several hundred thousand to several million years, depending on assumed permeability. These results suggest that a hydrothermal system induced by an impact event can remain active for sufficiently long periods of time to be biologically significant, supporting the idea that impact events may have played an important biological role, especially early in Earth's history. *INDEX TERMS:* 5420 Planetology: Solid Surface Planets: Impact phenomena (includes cratering); 8424 Volcanology: Hydrothermal systems (8135); 3210 Mathematical Geophysics: Modeling; 1829 Hydrology: Groundwater hydrology; *KEYWORDS:* Sudbury, impact cratering, crater cooling, hydrothermal systems, numerical modeling, astrobiology

Citation: Abramov, O., and D. A. Kring (2004), Numerical modeling of an impact-induced hydrothermal system at the Sudbury crater, *J. Geophys. Res.*, *109*, E10007, doi:10.1029/2003JE002213.

1. Introduction

1.1. Impact-Induced Hydrothermal Systems

[2] Current research suggests that impact-generated hydrothermal systems may have played an important role on early Earth. A dramatic increase in the number of impact events occurred at ~3.9 Ga [*Turner et al.*, 1973; *Tera et al.*, 1974; *Cohen et al.*, 2000; *Kring and Cohen*, 2002] and coincides remarkably well with the earliest isotopic evidence of life at ~3.85 Ga [*Mojzsis and Harrison*, 2000]. This period lasted 20 to 200 million years [*Ryder*, 1990; *Tera et al.*, 1974], during which time hydrothermal heat generated by impact events may have exceeded that generated by volcanic activity [*Kring*, 2000]. These impacts would have resurfaced most of the Earth and may have vaporized the Earth's oceans, virtually eliminating surface habitats while creating an abundance of subsurface ones [*Zahnle and Sleep*, 1997]. In addition, there is genetic evidence in the form of phylogenies that suggest that Archaea, Bacteria, and Eukarya have a common ancestor comparable to present-day thermophilic or hyperthermophilic organisms [e.g., *Pace*, 1997]. These lines of evidence suggest that impact-generated hydrothermal systems may have been important in the origin and evolution of early life [*Kring*, 2000] and deserve further study.

[3] Several hydrothermal systems associated with terrestrial impact craters have been identified based on mineralogical evidence. Examples of known systems include the ~24 km Haughton crater [*Osinski et al.*, 2001], the ~35 km Manson crater [*McCarville and Crossey*, 1996], the 80 km Puchezh-Katunki crater [*Naumov*, 1993, 2002], and the 150 to 250 km Sudbury crater [e.g., *Farrow and Watkinson*, 1992; *Ames et al.*, 1998]. In general, larger craters show more extensive hydrothermal alteration. Small, simple craters, such as the 1.2 km Meteor Crater in Arizona, typically have no evidence of hydrothermal activity. Impact-induced hydrothermal activity has been suggested for Martian craters as well [*Newsom*, 1980; *Allen et al.*, 1982; *Newsom et al.*, 1996].

[4] The primary heat sources driving a hydrothermal system associated with a complex impact crater are the

0148-0227/04/2003JE002213$09.00

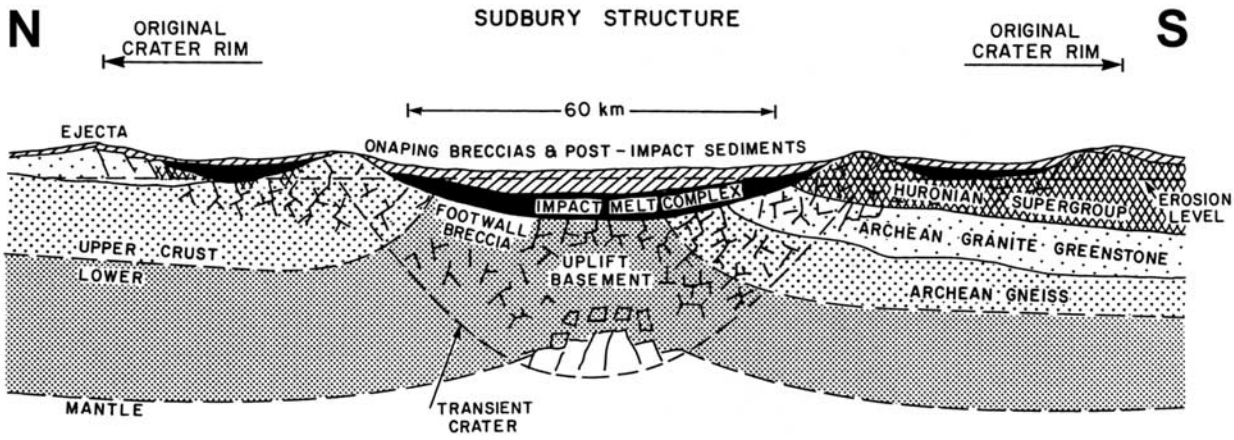

Figure 1. Schematic cross section of the Sudbury impact crater. The present level of erosion is indicated by a dashed line. Postimpact activity has masked much of these original relationships, replacing them with exposures of subsurface lithologies that were deformed by subsequent tectonic activity. From *Grieve et al.* [1991].

central uplift and the melt sheet, with the latter contributing ~10 to 100 times more energy [*Daubar and Kring*, 2001]. The lifetimes of hydrothermal systems in craters 20 to 200 km in diameter are 10^3 to 10^6 years if purely conductive cooling is assumed [*Daubar and Kring*, 2001; *Turtle et al.*, 2003]. In order to better constrain the expected lifetimes of these systems and further understand their mechanics, a finite difference computer simulation can be used to evaluate the additional effects of convective cooling. The results generated by a numerical simulation of the hydrothermal system at Sudbury crater are presented in this paper.

1.2. Sudbury Crater

[5] While the origin of the 15,000 km^2 Sudbury structure in Ontario, Canada, has been controversial for several decades, it is now largely accepted to be a remnant of a large impact crater [e.g., *Grieve et al.*, 1991]. Uranium-lead zircon dating by *Krogh et al.* [1984] places the formation of the Sudbury crater at 1.850 Ga. It is located on the Canadian Shield, at the present boundary of the Proterozoic Southern Province and the Archaean Superior Province. The Proterozoic supracrustal rocks belong to the Huronian Supergroup and have been dated to 2.5–2.4 Ga [*Krogh et al.*, 1984], while the Archaean rocks are mainly gneisses that are about 2.7 Ga old [*Krogh et al.*, 1984]. The Sudbury structure consists of the Sudbury Igneous Complex (SIC), now widely interpreted as a crystallized impact melt sheet [*Brockmeyer*, 1990; *Grieve et al.*, 1991], the footwall breccias underlying the melt sheet, and the Onaping breccias and postimpact sediments in the Sudbury Basin [*Dressler*, 1984a; *Giblin*, 1984] (Figure 1). The SIC occurs in the center of the Sudbury structure and at present is an elliptical body, ~60 km by 27 km, and 2.5 to 3.0 km thick, with an estimated volume of ~8000 to ~14,000 km^3 [*Grieve*, 1994]. The three lithological layers within the SIC are, from bottom to top, norite, quartz gabbro, and granophyre [e.g., *Dressler et al.*, 1992], which has been interpreted as evidence of melt sheet differentiation by fractional crystallization [e.g., *Therriault et al.*, 2002]. Brecciated basement rocks, including a zone of thermally metamorphosed heterolithic footwall breccia [e.g., *Dressler*, 1984b; *Dressler et al.*, 1992], are located directly below the SIC. Also, discontinuous, kilometer-sized bodies of the contact sublayer occur at the base of the SIC [e.g., *Naldrett et al.*, 1984]. This sublayer is mostly heterogeneous and characterized by abundant xenoliths and Cu-Ni sulfide mineralization. [e.g., *Prevec et al.*, 2000]. Most of the SIC is covered by up to 3 km of impact breccias and postimpact sedimentary deposits [*Pye et al.*, 1984; *Grieve et al.*, 1991; *Ivanov and Deutsch*, 1999]. These impact breccias and postimpact sediments overlying the SIC in the Sudbury Basin belong to the Whitewater Group, which consists of four formations, from oldest to youngest, the Onaping, Vermilion, Onwatin, and Chemselford [*Pye et al.*, 1984]. The Onaping formation is a 1.4 km thick sequence of fragmental and minor intrusive rocks, which are thought to represent fallback and washback breccia [*French*, 1967, 1968; *Peredery and Morrison*, 1984; *Dressler et al.*, 1996]. The Vermilion (5 to 50 m thick), Onwatin (600 to 1100 m thick), and Chemselford (600 to 850 m thick) formations are interpreted as postimpact sediments, with Vermilion being composed of carbonate, gray argillite, and chert; Onwatin being composed of conductive, carbonaceous, and sulfidic argillite; and Chemselford being composed of greywacke and minor siltstone [*Rousell*, 1984b; *Ames et al.*, 2002].

[6] Postimpact tectonic activity has deformed the Sudbury crater, giving it its present elliptical surface appearance. Seismic reflection studies by *Milkereit et al.* [1992] suggest that the deep geometry of the Sudbury structure is markedly asymmetric as well, which the authors interpreted to be the result of the 1.83 to 1.89 Ga Penokean orogeny or the 1.63 to 1.80 Central Plains orogeny. The timing of the deformation was further constrained by *Wu et al.* [1994] using high-resolution seismic reflection. This study found a lack of faults in the Chemselford turbidites, indicating that the Chemselford sediments postdate the latest major deformation of the Sudbury structure, constraining it to the Penokean orogeny. The original Sudbury crater has also been heavily eroded, resulting in the removal of the rim, the peak ring, and part of the melt sheet and the

overlying breccias, in effect providing a horizontal cross section of the crater interior. The extent of erosion is indicated by a dashed line in Figure 1.

[7] Estimates of the original rim-to-rim diameter of Sudbury crater, based primarily on the radial position of shock metamorphic effects, range from 150 to 250 km. *Lakomy* [1990] estimated the crater diameter at 180 to 200 km, while *Wichman and Schultz* [1993] estimated the original crater was at least ~180 km. *Grieve et al.* [1991] placed the original rim-to-rim diameter at 150 to 200 km, although a more recent compilation suggests it may have been as large as ~250 km [*Grieve et al.*, 1995]. For the purposes of the model presented in this paper, the original rim-to-rim diameter of the Sudbury crater has been conservatively estimated to be 180 km, which agrees well with hydrocode simulations of the Sudbury impact by *Ivanov and Deutsch* [1999].

[8] The Sudbury crater is also the site of the most extensive hydrothermal alteration known in a terrestrial impact crater [*Farrow and Watkinson*, 1992; *Ames et al.*, 1998, 2002], although similarly large hydrothermal systems may have existed in other large terrestrial craters such as the Chicxulub crater in Mexico [e.g., *Zürcher and Kring*, 2004]. The most prominent examples of hydrothermal alteration are found in the Onaping Formation, which overlies the melt sheet [e.g., *Ames and Gibson*, 1995]. The Onaping formation is subdivided into three members. The ~150 m thick Basal Member is the lowest layer; it is discontinuous and composed of a variety of monolithic and heterolithic breccias. The 200 to 700 m thick Gray Member overlies the Basal Member and consists of breccias and devitrified and recrystallized glasses. The uppermost layer is the 800 to 1200 m thick Black Member, which is composed of breccias similar to the Gray Member but also has chloritized shard-like fragments and carbonaceous material in its matrix [*Muir and Peredery*, 1984].

[9] Specific examples of hydrothermal alteration within the Onaping formation include, from base to top, basinwide, semiconformable zones of silicification, albitization, chloridization, calcitization, and complex feldspathization. Silicification occurs primarily in the Basal Member and is characterized by a higher-temperature quartz-epidote-clinopyroxene-pyrrhotite-chalcopyrite-sphalerite assemblage [*Ames et al.*, 2002]. The ~300 m thick albitization zone is located mainly in the Gray member, with the intensity of alteration locally increasing toward aphanitic dikes, fluidal breccia complexes, and crater floor fractures [*Ames et al.*, 2002]. Calcite alteration affects the upper 800 to 1000 m of the Onaping formation (mainly the Black Member) and is characterized by the replacement of vitric shards by calcite and chlorite [*Ames et al.*, 1998, 2002].

[10] The alteration patterns in the Onaping formation, and also in the overlying sediments of the Vermilion formation, are similar to those found at subseafloor hydrothermal systems [*Ames et al.*, 1998, 2002]. This implies that the Sudbury crater was at least partly submerged shortly after its formation, and the circulating fluids may have included seawater and deep formational brines [*Farrow and Watkinson*, 1997; *Ames et al.*, 1997]. The Sudbury structure is the host of world-class Ni-Cu-PGE ores, which occur in offset dikes of the melt sheet, embayments in the contact sublayer, and in the basement rocks. The hydrothermal system generated by the Sudbury impact remobilized some of the metals and redeposited them in breccias and fractures and may have contributed to the formation of Cu-precious metal-enriched ore bodies in the footwall [e.g., *Farrow and Watkinson*, 1997; *Molnár et al.*, 1999]. Hydrothermal alteration is restricted to the units comprising the Sudbury Structure, precluding the possibility of it being a more regional phenomenon. In addition, uranium-lead dating of hydrothermal titanites by *Ames et al.* [1998] produces an age similar to that of the SIC, indicating that the heat sources of the hydrothermal system were created by the Sudbury impact event.

2. Model

2.1. Computer Code HYDROTHERM

[11] The numerical code used to model the postimpact water and heat flow at Sudbury crater is a modified version of the publicly available program HYDROTHERM (source code available from authors). HYDROTHERM is a three-dimensional finite difference model developed by the U.S. Geological Survey to simulate water and heat transport in a porous medium [*Hayba and Ingebritsen*, 1994]. Its operating range is 0 to 1200°C and 0.5 to 1000 bars; however, in this work the upper temperature limit has been extended to 1700°C for the modeling of the impact melt sheet. It was not necessary to extend the thermodynamic properties of water to 1700°C because at those temperatures the melt is completely impermeable and has no water circulating through it. HYDROTHERM models both heat transport by circulating water and conductive heat flow through the rock matrix.

[12] HYDROTHERM's mode of operation can be outlined as follows. User inputs are used to calculate the initial pressure and enthalpy of water at every mesh element. Pressure and enthalpy were chosen as the dependent variables in HYDROTHERM's governing equations because they uniquely describe the thermodynamic state of the fluid under both single and two-phase conditions. A lookup table is interrogated by a bicubic interpolation routine [*Press et al.*, 1986] to obtain water density, viscosity, and temperature values, as well as the gradients of those values for each pressure-enthalpy pair. The code then solves the mass and energy conservation equations for every mesh element and time step, calculating water flux vectors and temperature distribution in the medium. Spatial derivatives in these equations are discretized by a finite difference algorithm. The mass and energy conservation equations, respectively, can be written as follows:

$$\partial[\Phi S_w\rho_w + \Phi S_s\rho_s]/\partial t - \nabla \bullet [kk_{rs}\rho_s/\mu_s \bullet (\nabla P - \rho_s g\nabla D)] - \nabla \bullet [kk_{rw}\rho_w/\mu_w \bullet (\nabla P - \rho_w g\nabla D)] - R_m = 0 \quad (1)$$

$$\partial[\Phi S_w\rho_w H_w + \Phi S_s\rho_s H_s + (1-\Phi)\rho_R H_R]/\partial t - \nabla \bullet [kk_{rs}\rho_s H_s/\mu_s \bullet (\nabla P - \rho_s g\nabla D)] - \nabla \bullet [kk_{rw}\rho_w H_w/\mu_w \bullet (\nabla P - \rho_w g\nabla D)] - \nabla \bullet (K_m\nabla T) - R_H = 0, \quad (2)$$

where Φ is porosity, S is volumetric saturation ($S_w + S_s = 1$), ρ is density, t is time, k is intrinsic permeability, k_r is relative

permeability ($0 \leq k_r \leq 1$), μ is dynamic viscosity, P is pressure, g is acceleration due to gravity, D is depth, H is enthalpy, K_m is the thermal conductivity of the medium, T is temperature, R_m and R_H are mass and energy source/sink flow rate terms, respectively, and the subscripts w, s, and R refer to liquid water, steam, and the rock matrix, respectively. The dependent variables in equations (1) and (2) are the pressure and enthalpy of the fluid. These strongly coupled and highly nonlinear equations are treated using the Newton-Raphson iteration, leading to a system of linear equations that are solved for each mesh element and time step. This approach was pioneered by *Faust and Mercer* [1977, 1979a, 1979b] and refined by *Hayba and Ingebritsen* [1994].

[13] HYDROTHERM has been previously used for scientific applications; in particular, it was successfully applied to hydrothermal systems of volcanic origin [*Hayba and Ingebritsen*, 1997] and putative hydrothermal systems at Martian impact craters [*Rathbun and Squires*, 2002].

[14] While HYDROTHERM is well suited for modeling impact-induced hydrothermal systems, it makes several assumptions that need to be addressed. Perhaps its most significant shortcoming for the purposes of this work is its inability to model brines. The program makes the assumption that the fluid is pure water, while the fluids circulating in hydrothermal systems generally contain some dissolved solids. It is also likely, since the Sudbury crater was formed in the proximity of a shoreline at the time of impact, that the primary circulating fluid was seawater. However, the thermodynamic properties of seawater at subcritical temperatures are sufficiently close to that of pure water for the purposes of this model, and this approximation has also been invoked previously for the modeling of deep-sea hydrothermal systems [e.g., *Travis et al.*, 1991]. At supercritical temperatures, the effect of solutes in H_2O is minimized by extremely low permeabilities at those temperatures [*Hayba and Ingebritesen*, 1997]. In other words, the differences in thermodynamic properties due to the presence of solutes in water become important mainly at the supercritical temperatures (>374°C), at which there is little flow. Another important assumption made by HYDROTHERM is that the rock and water are in a local thermal equilibrium. This assumption is valid if the fluid flow is relatively slow and steady. It breaks down in cases of very rapid transients: Water would have to pass through 500 m of rock (the vertical resolution of our model) without reaching equilibrium. Such transients are unlikely except perhaps in the very early stages of the system. HYDROTHERM also assumes that the ground remains fully saturated throughout the simulation, meaning that all pore spaces remain filled by water. Assuming that the depth of the water table at the time of impact was less than 250 m (half the vertical resolution of the model), this assumption should hold true, since the rim of the crater is essentially an overturned near-surface region. Subsequently, after the water has drained from the rim, its permeability and porosity are set to near-zero to simulate an unsaturated elevated surface.

2.2. Model Conditions

[15] Taking advantage of the impact crater's radial symmetry, we examine a vertical cross section from the center of the crater to beyond the outer rim. The area studied extends to 150 km in radius and 16.5 km vertically and includes the central melt sheet, peak ring, melt in the annular trough, crater rim, and part of the ejecta blanket. This is represented on a 75 × 33 grid, with a total of 2475 blocks, resulting in a horizontal resolution of 2 km and vertical resolution of 0.5 km.

[16] The upper boundary of the model represents a layer of cold breccia 500 m thick, with pressure and temperature held constant at 1 atm and 20°C. It is effectively an infinite source or sink of the fluid, donating or accepting water depending on underlying hydrologic conditions. It also functions as a heat sink; so when the thermal energy reaches the upper boundary, it is permanently removed from the system. This construct is reasonable in a rapidly convecting crater lake situation, where heat is rapidly removed from the upper surface layer, and water is freely exchanged. In addition, to account for the unusually thick breccia overburden (~1.4 km) over the Sudbury melt sheet, an additional 1 km of breccia with an elevated initial temperature (250°C) has been placed over the central melt sheet and the annular trough (Figure 2). The bottom boundary is impermeable with a constant basal heat flux of 42.5 mW m^{-2} to match the average continental geothermal gradient of 25°C km^{-1} [*Sclater et al.*, 1980]. The left-hand boundary of the model is the axis of symmetry and is thus impermeable and insulating. The right-hand boundary is permeable for both fluid and heat and is located sufficiently far away from the center of the crater that the temperatures are close to an average geothermal gradient.

3. Input Parameters

3.1. Topography

[17] Topography, both above and below the breccia lens, has a strong effect on fluid flow and it is included in the model. The Sudbury crater in its current state is extensively modified by erosional, tectonic, and depositional processes, making it difficult to reconstruct its initial topography. Seismic and gravity studies of a similarly sized ~180 km Chicxulub crater have shown a peak-ring structure [e.g., *Morgan et al.*, 1997; *Hildebrand et al.*, 1998], as was chosen for our model. While the horizontal positions of features such as the peak ring and the crater rim have been fairly well constrained by seismic and gravity studies, the topographic highs would have been subject to erosion after the formation of the crater, thus reducing vertical topography [*Morgan et al.*, 1997]. This holds true for other complex terrestrial impact craters, none of which are topographically pristine.

[18] Fortunately, good topography data are available for large samples of lunar [e.g., *Pike*, 1977] and Martian [*Garvin et al.*, 2002] craters. The recent data on large craters on Mars, acquired by the MOLA instrument on the Mars Global Surveyor spacecraft, are of very high quality but not readily applicable to fresh terrestrial craters, since craters on Mars have been degraded in various degrees by erosional and depositional processes. Therefore our Sudbury topographic model is based on the morphometry of lunar craters, summarized in Table 1. The chosen topographic parameters also correspond well to the hydrocode

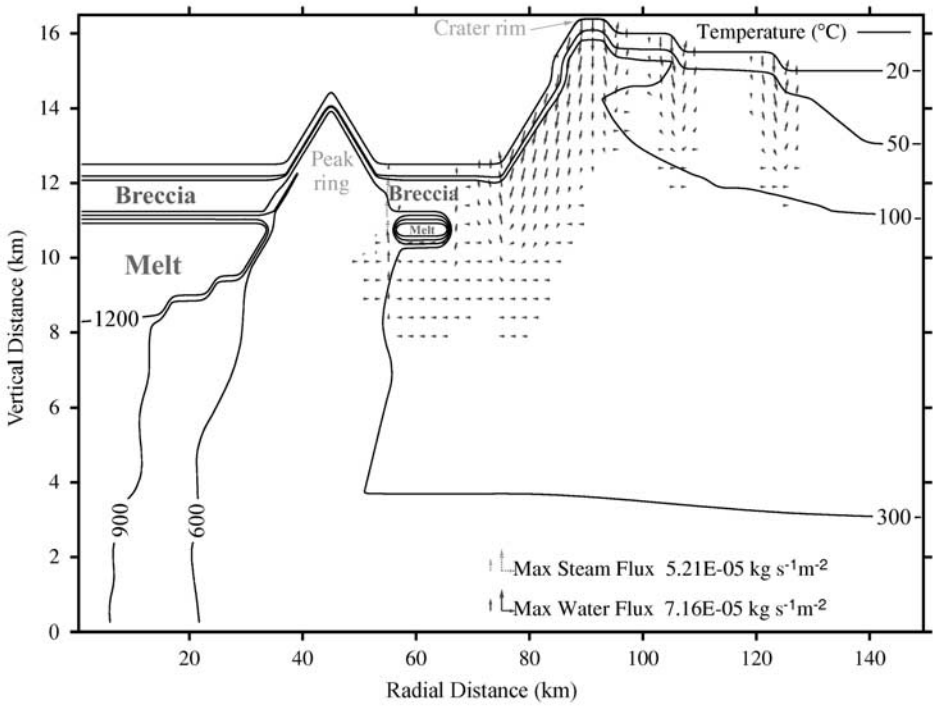

Figure 2. Model cross section shortly after the formation of the final crater, illustrating the draining of the rim. Surface permeability k_0 is 10^{-2} darcies. Solid arrows and dotted arrows indicate the water and steam fluxes, respectively. Solid lines are isotherms, labeled in degrees Celsius. The length of the arrows scales logarithmically with the flux magnitude. The maximum fluxes observed here are 7.16×10^{-5} kg s^{-1} m^{-2} for water and 5.21×10^{-5} kg s^{-1} m^{-2} for steam.

simulations of Chicxulub crater collapse by *Collins et al.* [2002].

3.2. Temperature Distribution

[19] In the initial stages of formation of a large crater such as Sudbury, part of the kinetic energy of an impacting body is converted into thermal energy of the target material by the process of shock heating. This process raises the temperature of the target material and melts a fraction of it. A fraction of the energy of the impactor is also converted into kinetic energy of the target material, resulting partly in the structural uplift of hot material from the lower crust to near-surface depths.

[20] These two processes have been successfully modeled by a hydrocode simulation of the Sudbury impact event [*Ivanov and Deutsch*, 1999]. The impactor was modeled as a stony spherical body 14 km in diameter traveling perpendicular to the ground with a velocity of 20 km s^{-1}. These parameters were chosen to fit the melt volume of 8000 km^3, as estimated by *Grieve and Cintala* [1992] for Sudbury crater. The postimpact temperature distribution generated by this hydrocode simulation is used as one of the starting conditions for our modeling.

[21] As previously mentioned, the geothermal gradient chosen for our simulations is 25°C/km, which is the current average continental geothermal gradient on Earth [*Sclater et al.*, 1980], plus ~10% to account for a higher geothermal gradient at 1.85 Ga. At that time, the geothermal gradient was ~10% higher than present-day because of higher concentrations of radioisotopes [*Ganguly et al.*, 1995].

3.3. Pressure Distribution

[22] The initial pressure distribution is calculated by HYDROTHERM hydrostatically, that is:

$$P_i(z) = P_0 + \rho g z, \tag{3}$$

where P_0 is atmospheric pressure (1 atm), ρ is rock density (2700 kg m^{-3}), g is Earth's gravitational acceleration (9.81 m s^{-2}), and z is depth below the surface.

3.4. Melt Sheet Properties

[23] The melt sheet volume of 8000 km^3 was chosen for consistency with the *Ivanov and Deutsch* [1999] temperature

Table 1. Parameters Used for Reconstruction of the Original Topography of Sudbury Crater, With Diameter D = 180 km[a]

Parameter	Dependence on Rim-to-Rim Diameter D, km	Source
Crater depth	$1.044\ D^{0.301}$	*Pike* [1977]
Crater floor diameter	$0.19\ D^{1.25}$	*Pike* [1977]
Peak ring diameter	$0.5\ D$	*Wood and Head* [1976]
Peak ring height	3	*Hale and Grieve* [1982]
Peak ring thickness	$0.11\ D$	*Pike* [1985]
Rim height	$0.236\ D^{0.399}$ $((0.5D)^3/r^3)$	*Pike* [1977], *Melosh* [1989]

[a]The variable r is the distance from the center of the crater. All parameters were obtained from morphometric studies of lunar craters. These parameters describe the topography of the Sudbury crater before an additional 1 km of breccia was added above the melt. After *Melosh* [1989].

distribution and impactor properties. This value also corresponds well to the melt sheet volume of 10^4 km^3 estimated by *Wu et al.* [1995]. The geometry of the central melt sheet was chosen to fill a bowl-shaped cavity formed within the peak ring during crater collapse [e.g., *Melosh*, 1989], and the initial temperature was set to 1700°C, as estimated by *Ivanov and Deutsch* [1999]. In complex peak ring craters, substantial melt has also been observed between the peak ring and the final crater rim (as seen at Chicxulub) [*Kring and Boynton*, 1992]. Consequently, we have placed a small amount of melt ($\sim$1.9 km^3, consistent with Chicxulub observations), which we refer to as the small melt sheet, in the annular trough between the peak ring and the crater rim. The melt sheet volume of 8000 km^3 includes the melt in the annular trough as well as the central melt sheet.

[24] The issue of possible melt sheet convection was examined. In order for a true convection cell to form, an independent heat source needs to be present below or within the convecting material, which is not the case for impact melt sheets. Thus the main process for long-term mixing of the melt sheet is slow overturn, where denser material from the near-surface layers sinks and is replaced by warmer material from below. This process is unlikely to have significantly contributed to the cooling of the Sudbury melt sheet because of substantial viscous damping [*Onorato et al.*, 1978] and the presence of a 1.4 km layer of insulating breccia, and is not modeled here.

[25] The latent heat of fusion is included in the model using the approximation of *Jaeger* [1968], after *Onorato et al.* [1978], replacing the heat capacity C_p in the temperature range between the liquidus (T_L) and the solidus (T_S) with

$$C_p' = C_p + L/(T_L - T_S). \tag{4}$$

[26] Here L is the latent heat of fusion of diopside, 421 kJ kg^{-1}. The liquidus and solidus temperatures of 1450 K (1177°C) and 1270 K (997°C), respectively, have been estimated for the Sudbury melt sheet by *Ariskin et al.* [1999] and used by *Ivanov and Deutsch* [1999] for thermal modeling of the Sudbury crater. The liquidus temperature of 1177°C agrees well with a liquidus temperature range of 1115°C to 1125°C calculated by *Ames et al.* [2002].

3.5. Rock Parameters

[27] The target rocks of the Sudbury impact were geologically complex (Figure 1), consisting of metasedimentary and metavolcanic rocks of the Huronian supergroup and Archaean granite-greenstone and gneissic lithologies [*Rousell*, 1984a; *Grieve et al.*, 1991]. The original depth and position of these layers within the Sudbury crater is not fully constrained [*Wu et al.*, 1995] and the layers are not radially symmetric, making them difficult to model. Thus the model crater has been approximated as being petrologically homogenous, with rock density, heat capacity, and thermal conductivity listed in Figure 2 being good approximations to the Sudbury lithologies.

[28] The porosity in our model decreases exponentially with depth, accounting for the closing of pore spaces by lithostatic pressure, following the approach suggested by *Binder and Lange* [1980] for the lunar crust:

$$\Phi(z) = \Phi_0 \exp(-z/K), \tag{5}$$

where Φ_0 is surface porosity and K is the porosity decay constant. The depth z is measured with respect to local topography not the preimpact surface level. Since the bulk density of the lunar crust is comparable to that of the Earth, the inferred value of the lunar porosity decay constant K ($\sim$6.5 km) can be gravitationally scaled to get the corresponding value of the Earth [*Clifford*, 1993]:

$$K_{\text{Earth}} = 6.5 \text{ km}(g_{\text{Moon}}/g_{\text{Earth}}) = 1.07 \text{ km} \tag{6}$$

where g_{Moon} (1.62 m s^{-2}) and g_{Earth} (9.81 m s^{-2}) are the gravitational accelerations at the surface of the Moon and Mars, respectively. The surface porosity Φ_0 used in this model is 20%, consistent with measured porosities of lunar impact breccias [*Warren and Rasmussen*, 1987].

[29] It is reasonable to assume that the number of fractures in an impact crater decreases with depth [*Melosh*, 1989], and thus permeability in our model decays exponentially with depth similarly to porosity. It is also a function of temperature, approximating the effect of the brittle/ductile transition at about 360°C [*Fournier*, 1991] by log linearly decreasing permeability with increasing temperature between 360°C and 500°C:

$$\begin{aligned} k(z) &= k_0 \exp(-z/K) && T < 360^\circ\text{C}, \\ \log k(z,T) &= \frac{\log k(z) + 11}{500 - 360}(500 - T) - 11 && 360 \le T \le 500^\circ\text{C}, \\ k &= 10^{-11}\text{darcies} && T > 500^\circ\text{C}. \end{aligned} \tag{7}$$

[30] The surface permeability k_0 of crystalline rocks such as those present at the Sudbury site varies widely, depending on fracture frequency and width. *Brace* [1980, 1984] conducted in situ measurements of crystalline rocks, describing a large-scale permeability that ranges from 10^{-1} to 10^{-6} darcies, with an average value of $\sim 10^{-3}$ darcies for the Earth's crust. This value agrees well with the average permeability value derived from earthquake migration and other large-scale crustal phenomena. However, as inferred from negative gravity anomalies and low seismic velocities [e.g., *Kahle*, 1969; *Hildebrand et al.*, 1998], rocks beneath terrestrial impact craters are fractured to a higher degree than the surrounding crust, resulting in higher permeability. *Hanson* [1995] estimates a midrange value for fractured crystalline rocks at $\sim 10^{-1}$ darcies. To account for fracture closing due to hydrothermal mineralization in an approximate way, we use a value of 10^{-2} darcies in our model, which is a log average between the mean crustal permeability and midrange permeability in broken crystalline rocks. However, since this parameter has important effects on the dynamics and duration of a hydrothermal system, several values of k_0 were investigated in this study, including 10^{-3} darcies (mean crustal) and 10^{-1} darcies (broken crystalline).

[31] The porosity and permeability of the upper layer of breccia are assumed to be constant at Φ_0 and k_0, respectively. Rock density, thermal conductivity, and heat capacity were taken directly from the Sudbury impact simulations by *Ivanov and Deutsch* [1999] and remain constant throughout

Table 2. Rock Parameters Used in the Model

Parameter	Value	Units
Porosity	$f(z)$, 20% at the surface	unitless
Permeability	$f(z, T)$, 0.01 at the surface[a]	darcies
Thermal conductivity	1.7	W m^{-1} K^{-1}
Heat capacity	1050	J kg^{-1} K^{-1}
Density	2700	kg m^{-3}

[a]Value 0.01 unless otherwise indicated.

the simulations. All rock parameters used in this work are summarized in Table 2.

3.6. Crater Lake Formation

[32] A cross section of the Sudbury complex shortly after the formation of the final crater is shown in Figure 2. The rim of the crater is essentially an overturned near-surface region and is assumed to be saturated with water. Water in the rim is seen rapidly draining into the crater basin shortly after the formation of the crater. The subsequent water flux through the rim due to rainfall is insignificant compared to the fluxes in an active hydrothermal system, and thus the rim is made impermeable for the duration of the simulation. The groundwater table is assumed to be roughly at the depth of the original surface, at a vertical distance of 14.5 km in the model. In the absence of a marine incursion, groundwater would slowly seep into the depression created by the Sudbury impact, eventually filling it with water approximately to the level of the preimpact water table. We can roughly estimate the timescale for crater lake formation by measuring the net water influx into the crater and assuming that the rate of precipitation is equal to the rate of evaporation in the crater basin. Using this method, we estimate crater lake formation in ~10 to 1000 years after the impact for surface permeability values of 10^{-1} to 10^{-3} darcies, respectively.

[33] Additionally, there is physical evidence indicating that the Sudbury crater contained water for a large part of its history and that the crater was filled shortly after the impact. This evidence includes extensive sediments overlying the crater floor, comprising the Vermilion and the Onwatin Formations [*Rousell*, 1984b]. The Vermilion formation, which has Cu-Pb-Zn mineralization, appears to have been deposited while the hydrothermal system was still active [*Rousell*, 1984c, *Ames*, 2002], indicating an early flooding of the crater basin. In addition, the Sudbury impact occurred in a coastal or shallow marine environment, and the crater may have been flooded almost immediately by impact-generated tsunami waves, producing the well developed bedding seen in the Black member of the Onaping formation [*Peredery*, 1972; *Peredery and Morrison*, 1984]. An early incursion into the crater from the surrounding sea would have enhanced the fill rate estimated above from groundwater flow. Consequently, a crater lake has been incorporated into our model immediately after crater formation. While the actual process of filling the crater basin with water to a final depth of ~3 km could have taken over 10^3 years, this time period is insignificant in comparison with the overall hydrothermal system lifetime. The crater lake is set to a constant temperature (20°C), which is reasonable considering that the lake would be in a state of rapid convection because of heating from below.

4. Results

4.1. Hydrothermal System Mechanics and Lifetimes

[34] The results of a numerical simulation of the hydrothermal system at the Sudbury crater are shown in Figure 3. At 4000 years, the changes in the thermal state of the system since crater formation (Figure 2) are most apparent at the small melt sheet, which has reached its liquidus temperature and is undergoing crystallization. The temperature of the outer edge of the peak ring has decreased sufficiently to allow water to flow through it, and it is the site of a convective cell. The highest fluxes are observed in this region. Colder fluid enters near the base of the peak ring and is subsequently heated and transported upward. A similar effect is also seen at the far wall of the crater but results in smaller fluxes as a result of lower temperatures. Another convective cell is driven by the small melt sheet and results in water discharge through the breccias above it. There is also some water flow underneath the melt sheet toward the peak ring to feed the vigorous outflow located there. Relatively large quantities of steam are also seen emanating from the upper part of the peak ring, originating near the critical point of water at 374°C. Crystallization of the melt, and thus this stage, may have occurred more quickly but would not significantly affect the overall lifetime of the hydrothermal system because it is dominated by the thermal input of the central melt sheet.

[35] At 20,000 years, there are apparent changes in the temperature contours due to the upward flow of warmer fluids and downward flow of colder fluids. The small melt sheet has completely solidified, but a remnant (and still impermeable) hot spot with a mean temperature of 430°C remains and drives a prominent upwelling approximately 8 km across in this area. Downward flow is observed on either side of the former melt sheet, feeding the upwelling. Another prominent change from the earlier time step is the temperature of the peak ring, which has decreased sufficiently to allow water flow through most of the structure. There is some supercritical steam being produced within the

Figure 3. Results of the numerical simulation of the hydrothermal system at Sudbury crater. Surface permeability k_0 is 10^{-2} darcies. The left panel shows color-coded temperature fields, and the right panel displays fluid flux vectors. Black lines are isotherms, labeled in degrees Celsius, and blue and red arrows represent water and steam flux vectors, respectively. The length of the arrows scales logarithmically with the flux magnitude, and the maximum value of the flux changes with each plot: (a) 4000 years, maximum water flux = 1.41×10^{-5} kg s^{-1} m^{-2} and maximum steam flux = 3.78×10^{-8} kg s^{-1} m^{-2}; (b) 20,000 years, maximum water flux = 1.15×10^{-5} kg s^{-1} m^{-2} and maximum steam flux = 4.31×10^{-7} kg s^{-1} m^{-2}; (c) 200,000 years, maximum water flux = 1.13×10^{-5} kg s^{-1} m^{-2} and maximum steam flux = 1.26×10^{-12} kg s^{-1} m^{-2}; (d) 2×10^6 years, maximum water flux = 4.16×10^{-6} kg s^{-1} m^{-2}.

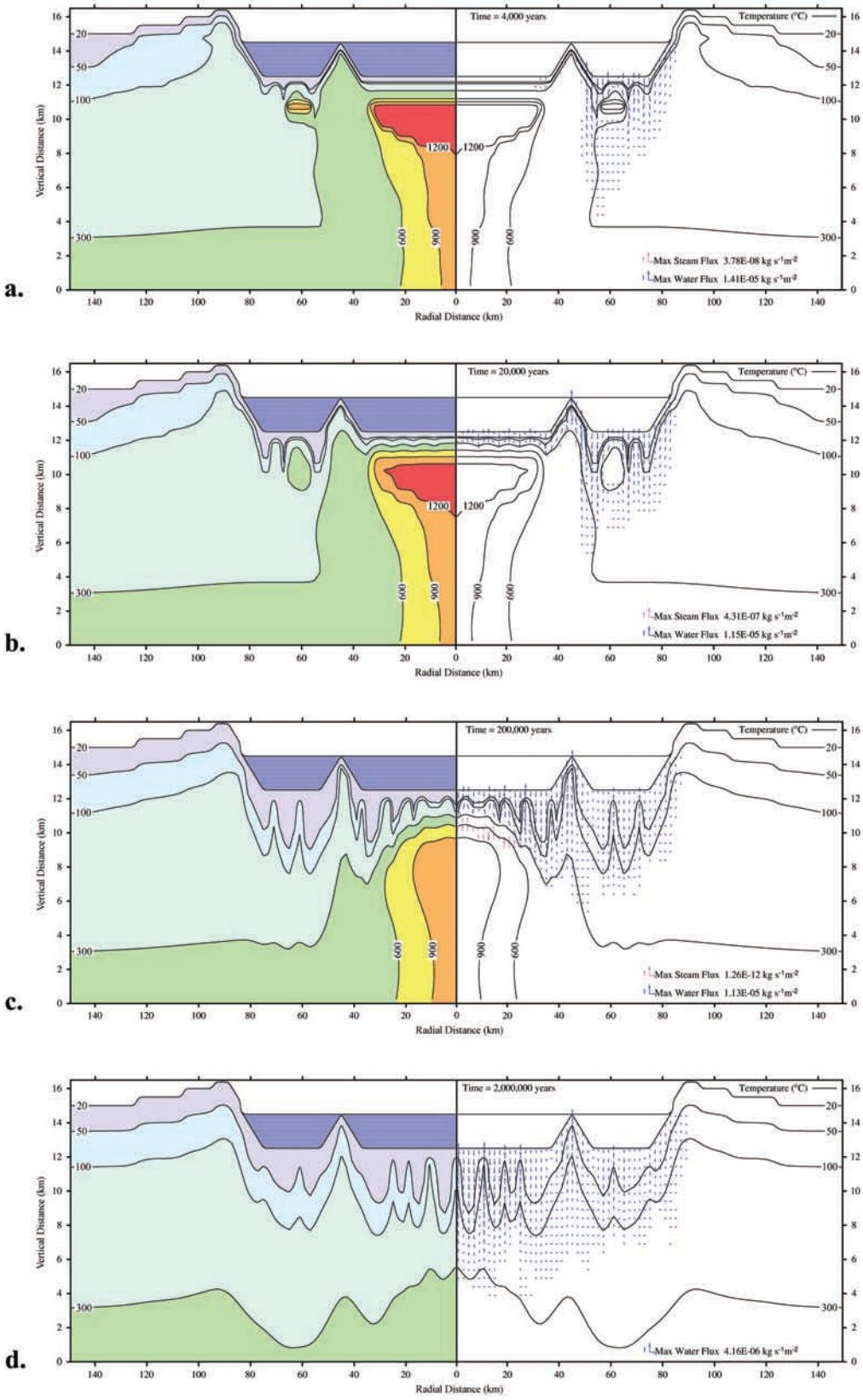
a.
Time = 4,000 years
Temperature (°C)
Max Steam Flux 3.78E-08 kg s⁻¹m⁻²
Max Water Flux 1.41E-05 kg s⁻¹m⁻²
b.
Time = 20,000 years
Temperature (°C)
Max Steam Flux 4.31E-07 kg s⁻¹m⁻²
Max Water Flux 1.15E-05 kg s⁻¹m⁻²
c.
Time = 200,000 years
Temperature (°C)
Max Steam Flux 1.26E-12 kg s⁻¹m⁻²
Max Water Flux 1.13E-05 kg s⁻¹m⁻²
d.
Time = 2,000,000 years
Temperature (°C)
Max Water Flux 4.16E-06 kg s⁻¹m⁻²
Vertical Distance (km)
Radial Distance (km)

Figure 3

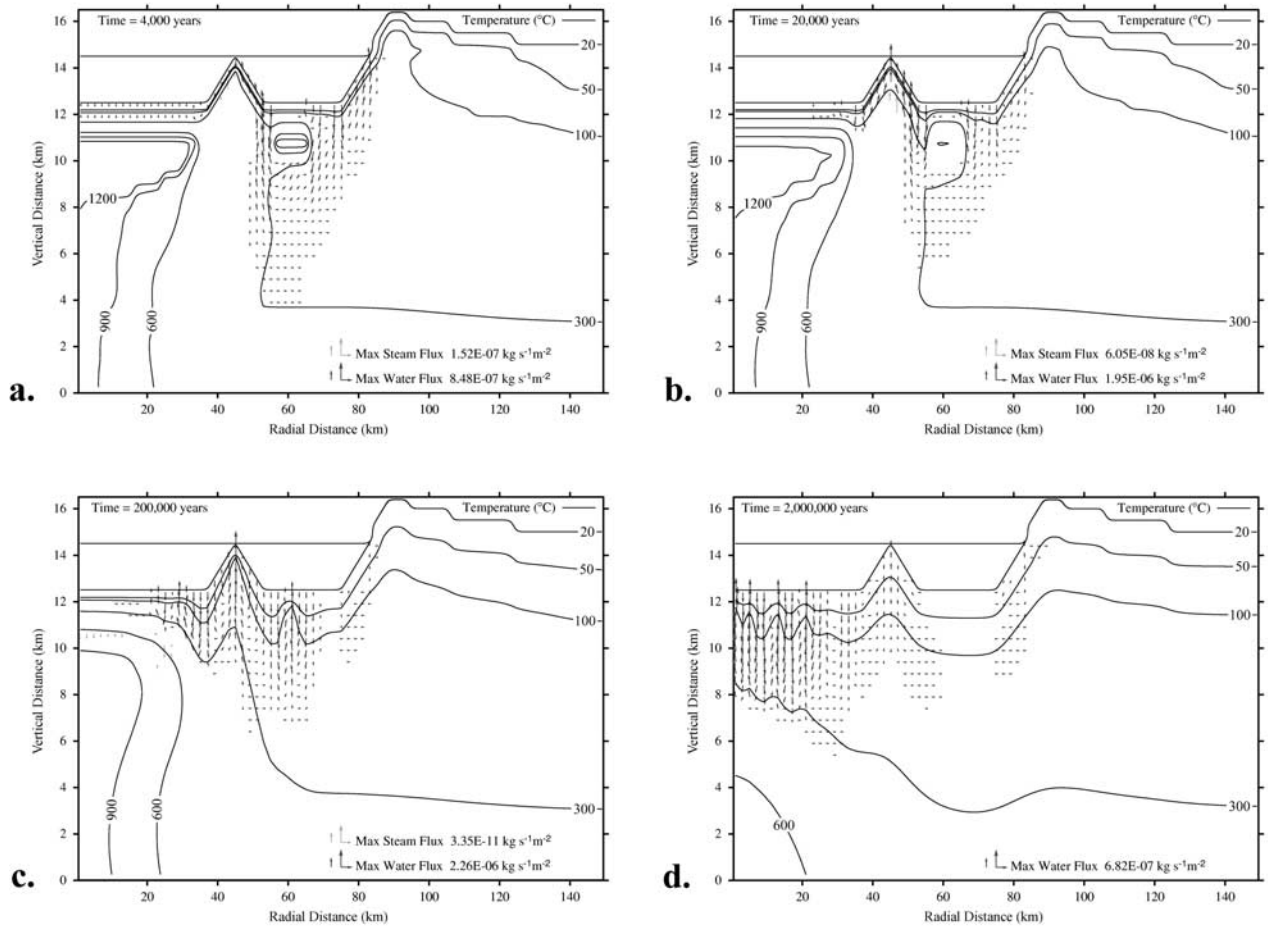

Figure 4. Numerical simulation of the hydrothermal system at Sudbury crater with surface permeability k_0 set to 10^{-3} darcies. Solid lines are isotherms, labeled in degrees Celsius, and solid and dotted arrows represent water and steam flux vectors, respectively. The length of the arrows scales logarithmically with the flux magnitude, and the maximum value of the flux changes with each plot: (a) 4000 years, maximum water flux = 8.48×10^{-7} kg s^{-1} m^{-2} and maximum steam flux = 1.52×10^{-7} kg s^{-1} m^{-2}; (b) 20,000 years, maximum water flux = 1.95×10^{-6} kg s^{-1} m^{-2} and maximum steam flux = 6.05×10^{-8} kg s^{-1} m^{-2}; (c) 200,000 years, maximum water flux = 2.26×10^{-6} kg s^{-1} m^{-2} and maximum steam flux = 3.35×10^{-11} kg s^{-1} m^{-2}; (d) 2×10^{6} years, maximum water flux = 6.82×10^{-7} kg s^{-1} m^{-2}.

peak ring at the critical temperature of water, but it condenses before reaching the surface. The high temperatures within the peak ring are driving an upward flow, which is being concentrated at the tip of the ring. The largest fluxes in the current time step are seen in this area. High water fluxes in this area are observed in subsequent time steps; however, the nature of this flow might be different if the peak ring is not fully submerged. The upward water flow along the wall of the crater continues as before and only changes in magnitude, not character, in subsequent time steps. This flow would likely migrate upward along the faults in the modification zone of the crater. The central melt sheet has undergone some cooling but remains largely molten and completely impermeable. However, there is some circulation through the permeable breccias above it.

[36] At 200,000 years the small melt sheet has completely cooled, but the two upward flows it drove remain active. This is because these flows are self-sustaining; they transport heat closer to the surface, maintaining a warm area that continues to drive the flow. The upwelling at the peak ring continues as before. The central melt sheet has fully crystallized and is partly permeable, allowing several convection cells to form in its upper region. The magnitudes of water fluxes continue to decrease, with the largest flux observed here being ~20% smaller than those observed early in the system (4000 years).

[37] At 2 million years, temperatures have returned close to a geothermal gradient. The central melt sheet has cooled completely, and only a hint of the temperature increase due to the central uplift remains. There are still several "fossil" flows still active, most notably at the former central melt sheet and the peak ring, but the largest flux here is 3.5 times smaller than those present early in the system at 4000 years. However, it is possible that the fluxes would be even smaller as a result of fracture closing due to hydrothermal mineralization, so perhaps the corresponding 2 Ma time step in Figure 4, where the permeability is 10^{-3} darcies, is a better representation of the system at this stage. Owing to

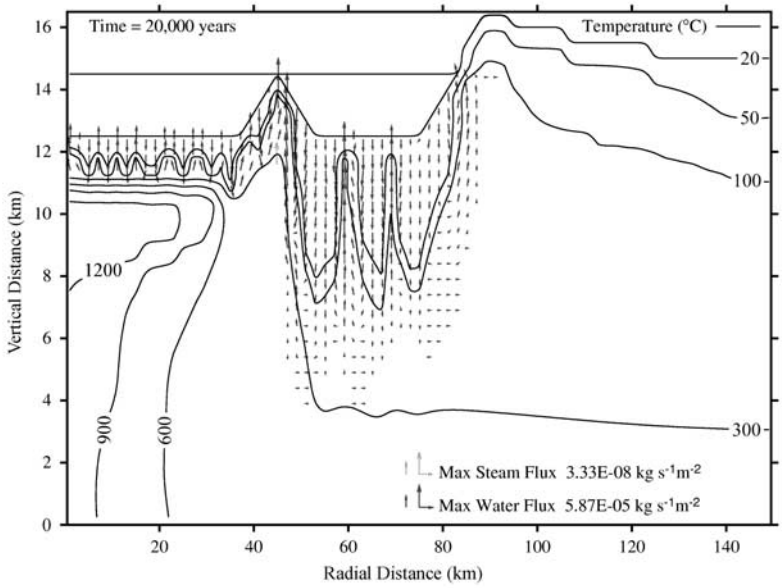

Figure 5. The state of the hydrothermal system at Sudbury crater with surface permeability k_0 set to 10^{-1} darcies at 20,000 years. Solid lines are isotherms, labeled in degrees Celsius, and solid and dotted arrows represent water and steam flux vectors, respectively. The length of the arrows scales logarithmically with the flux magnitude, and the maximum value of the flux changes with each plot. The maximum fluxes observed here are 5.87×10^{-5} kg s^{-1} m^{-2} for water and 3.33×10^{-8} kg s^{-1} m^{-2} for steam.

the low volumes of water in these flows and the thickness of colder rocks they must traverse, in most cases the water would be expected to cool off completely before reaching the surface.

4.2. Effects of Permeability

[38] In addition to the main simulation with a surface permeability k_0 of 10^{-2} darcies, values of 10^{-3} darcies and 10^{-1} darcies were tested, corresponding to the average crustal permeability and a midrange value for fractured crystalline rocks, respectively. Figure 4 illustrates the differences in flow characteristics and thermal evolution of Sudbury crater with a k_0 value of 10^{-3} darcies.

[39] At 4000 years, the overall temperatures are noticeably higher, particularly near the small melt sheet. The overall water flow characteristics are similar, but the fluxes involved are over an order of magnitude smaller. The two main differences are the absence of upwelling at the right of the small melt sheet and a virtual lack of flow through the breccias above the small melt sheet. The latter is explained by higher temperatures cutting off permeability, and the former is explained by a proportionally greater water flow underneath the small melt sheet toward the base of the peak ring to feed the strong upwelling there. At 20,000 years, the hot spot remaining at the site of the small melt sheet has a central temperature of over 600°C and is hotter than before, resulting in a larger impermeable volume. A more notable difference is in the shape of temperature contours, which here are virtually unchanged by long-lived vertical water flows. The peak ring is significantly hotter, and, as before, large quantities of steam are internally generated. The breccias above the central melt sheet are still largely too hot to permit flow. At 200,000 years, the main difference is the lack of convection above the hot spot in the central part of the crater. This is due to significantly higher temperatures that do not permit flow, except in the near-surface region. The convection cells in that area do eventually develop when temperatures decrease to acceptable levels. Another difference is that the number of active convection cells is significantly smaller. At 2 million years, the temperatures have returned to near-geothermal levels, but are still significantly higher near the center of the crater. This was to be expected since less heat was removed by circulating water than in the case of higher permeability. Perhaps more noticeably, the shapes of the temperature contours are virtually unaffected by vertical water movement, except near the center of the crater, where active convection still continues. Elsewhere in the model, some water circulation continues, but the flux magnitudes are essentially negligible. As mentioned before, this may be a better representation of the system at this stage, accounting for fracture closing due to hydrothermal mineralization.

[40] As expected, a system with a surface permeability k_0 of 10^{-1} darcies cools significantly faster, and the shape of temperature contours is dramatically altered by long-lived vertical water flows. Figure 5 shows the state of this high-permeability hydrothermal system at 20,000 years. Note that unlike the lower permeability cases previously examined, the remnant hot spot from the small melt sheet is no longer in existence, and overall the system is significantly cooler. Three large upwellings are present; one at the site of the former small melt sheet and one at the peak ring and one in the modification zone, with maximum water fluxes $\sim$5 times greater than those for the k_0 of 10^{-2} darcies. Fluid convection in the breccias overlying the central melt sheet also starts sooner than in the lower-permeability runs.

[41] Defining the "lifetime" of a hydrothermal system is somewhat subjective, as there is no clear transition between

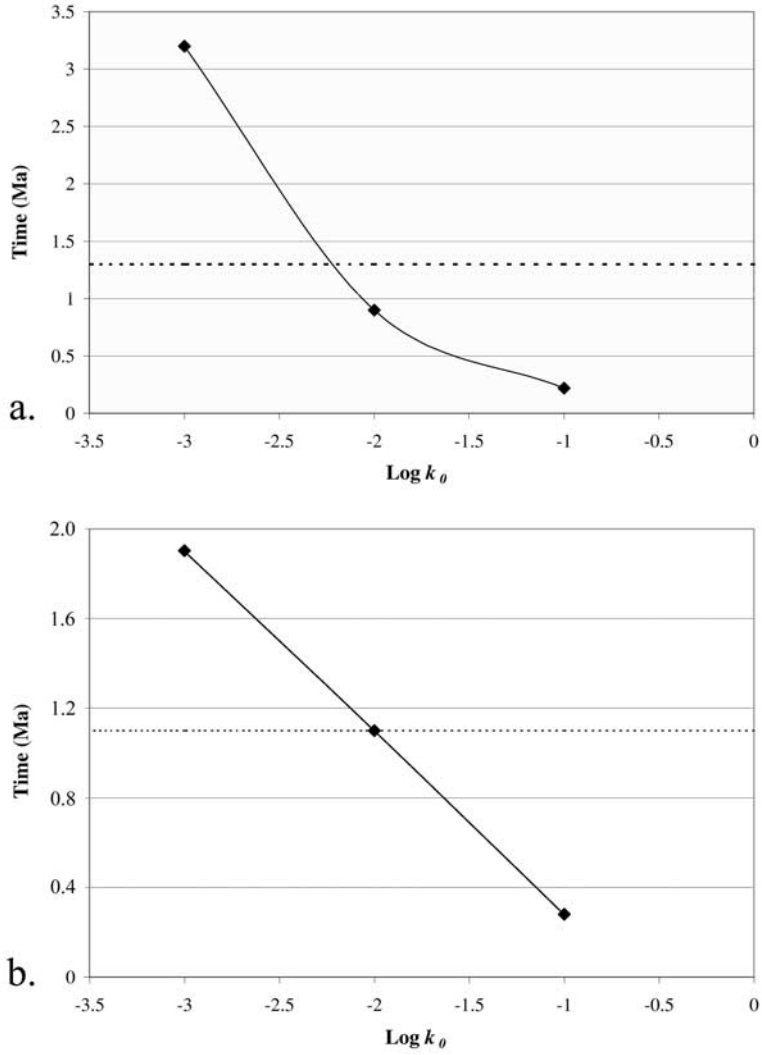

Figure 6. Effects of permeability on the lifetime of the Sudbury hydrothermal system. Here k_0 denotes surface permeability. The dashed line indicates system lifetime in the absence of water flow. (a) Breccia layer 1500 m thick. (b) Breccia layer 500 m thick.

an active and inactive system. We conservatively define the lifetime as the time it takes for the system to cool below 90°C (200% of the geothermal level) within 1 km of the surface everywhere in the model. Figure 6a shows the dependence of system lifetime on surface permeability k_0, with estimated lifetimes of 0.22 Ma for a k_0 of 10^{-1} darcies, 0.90 Ma for a k_0 of 10^{-2} darcies, and 3.2 Ma for a k_0 of 10^{-3} darcies. These values are within the range of inferred durations of terrestrial hydrothermal systems of volcanic origin, such as the ones at Round Mountain, Nevada (~0.1 Ma) [*Henry et al.*, 1997], Yellowstone, Wyoming (~0.6 Ma, still active) [*Fournier*, 1989], Geysers, California (~1.4 Ma, still active) [*Donnelly-Nolan et al.*, 1993], and Bingham, Utah (~2.1 Ma) [*Warnaars et al.*, 1978]. However, the area of hydrothermal activity at Sudbury crater (~25,000 km^2) would have been far greater than that of any known hydrothermal system of volcanic origin on Earth. At the interval examined (10^{-3} to 10^{-1} darcies) the lifetime decreases with the log of k_0, implying that the degree of convective cooling increases as more water is circulated through the system. However, note that the system lifetime in the absence of fluid flow (see section 4.3), indicated by a dashed line, is significantly less than that for the k_0 of 10^{-3} darcies. This indicates that at lower permeabilities, water flow can actually increase system lifetime by transporting heat from the interior to the near-surface regions. At higher permeabilities, however, this effect is negated by the overall rapid cooling of the system.

4.3. Effects of Breccia Thickness

[42] The nonlinearity of the lifetime/permeability curve seen in Figure 6a is due mainly to the unusually thick breccia layer (1500 m) overlying the melt sheet. To illustrate this point, a simulation with a reduced breccia thickness of 500 m was performed (Figure 6b). The thicker breccia sheet provides additional insulation, and the crater cools slower by pure conduction as seen by comparing the location of the dashed line in Figures 6a and 6b. However, the thick breccia layer has a greater importance, because of its role as a highly permeable matrix for fluid circulation. At low

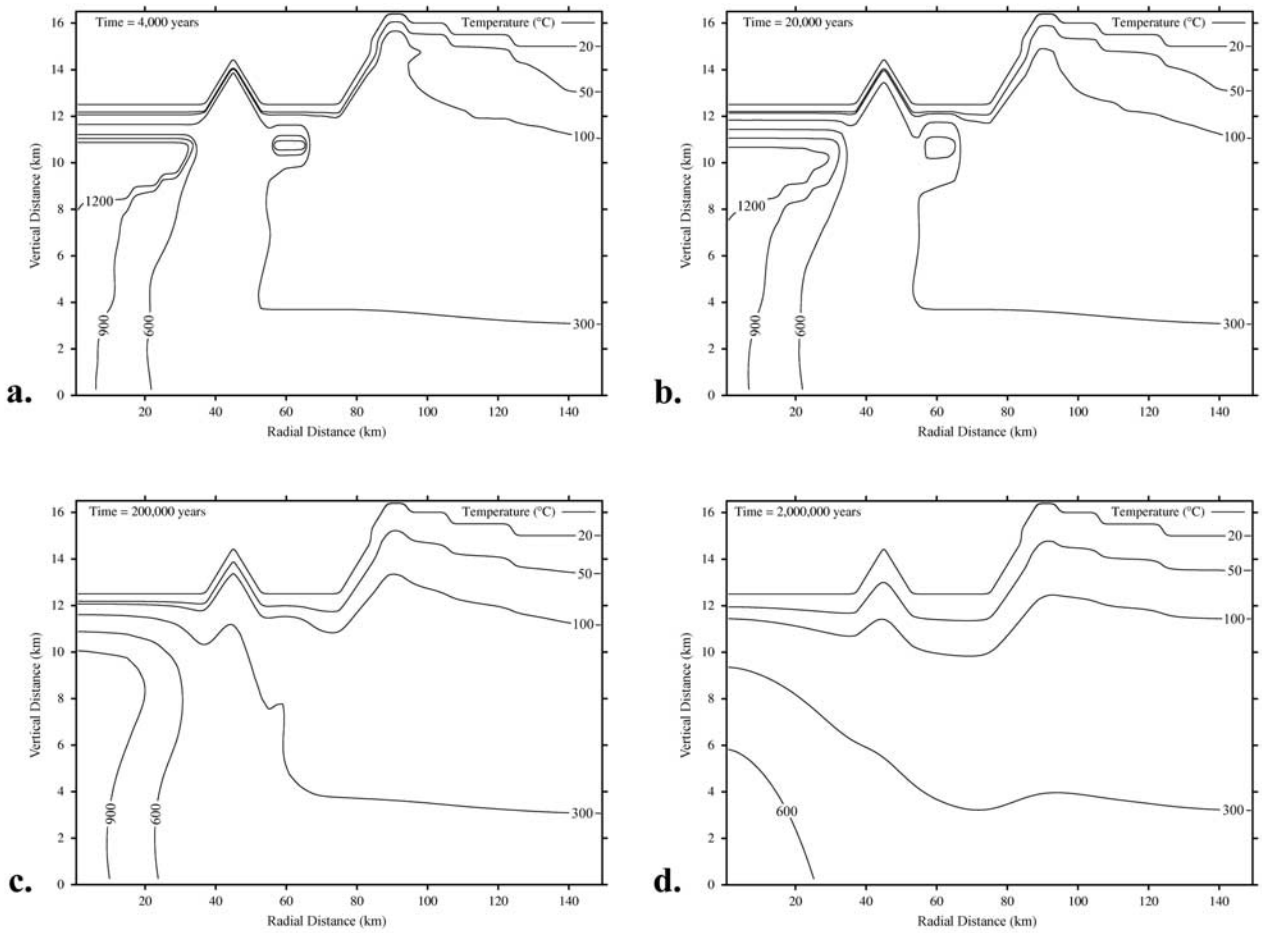

Figure 7. Thermal evolution of Sudbury crater without the presence of water (conductive cooling only). Black lines represent isotherms, which are labeled in degrees Celsius.

permeability (10^{-3} darcies) the crater cools slowly while some of the internal heat is transported by water to the near-surface in several parts of the model, resulting in a very long lifetime. At midrange and high permeabilities (10^{-2} and 10^{-1} darcies), on the other hand, large amounts of water circulating through the thick sheet of highly permeable breccia quickly cool the near-surface regions, lowering system lifetimes.

4.4. Heat Transport in the Absence of Fluid Flow

[43] By setting permeability and porosity to zero, HYDROTHERM can be used to model postimpact cooling with purely conductive heat transport. Figure 7 shows numerical modeling results of the thermal evolution of Sudbury impact crater in the absence of fluid flow. Not surprisingly, it is most similar to the low-permeability case of $k_0 = 10^{-3}$ darcies, because there is no water flow to alter the temperature contours. The overall system cooling rate is the slowest of all cases examined, however, some near-surface regions are warmer in the low-permeability case because of the upward transport of heat by water. The central melt sheet completely crystallizes by 130,000 years, which is similar to 97,000 years calculated by a thermal model of *Prevec and Cawthorn* [2002]. The longer time to crystallization in our model can be explained by the inclusion of the heat from the central uplift. The overall results of this simulation are similar to those of an analytical solution for conductive cooling of a generic crater of the same size [*Daubar and Kring*, 2001] and a numerical model of conductive cooling of a similarly sized Vredefort impact crater by *Turtle et al.* [2003].

4.5. Effects of Model Depth

[44] The optimal depth of the model was an issue of some concern, requiring a balance of computational considerations, such as longer run times due to an increased cell number, and the need to include additional heat from the central uplift found deeper in the model. It was found by trial and error that extending the depth of the model beyond 14.5 km has no appreciable effect on near-surface temperatures, water circulation, and the lifetime of the system as we define it.

5. Discussion

[45] The hydrothermal system modeled in this paper can produce the wide variety of mineral assemblages observed at Sudbury crater. The initial temperatures within much of the basin, in particular, near the small melt sheet, the peak ring, and the central melt sheet, are more than sufficient for high-temperature alteration processes to occur. For example, rocks of the lower Onaping formation (the lower 300–500 m

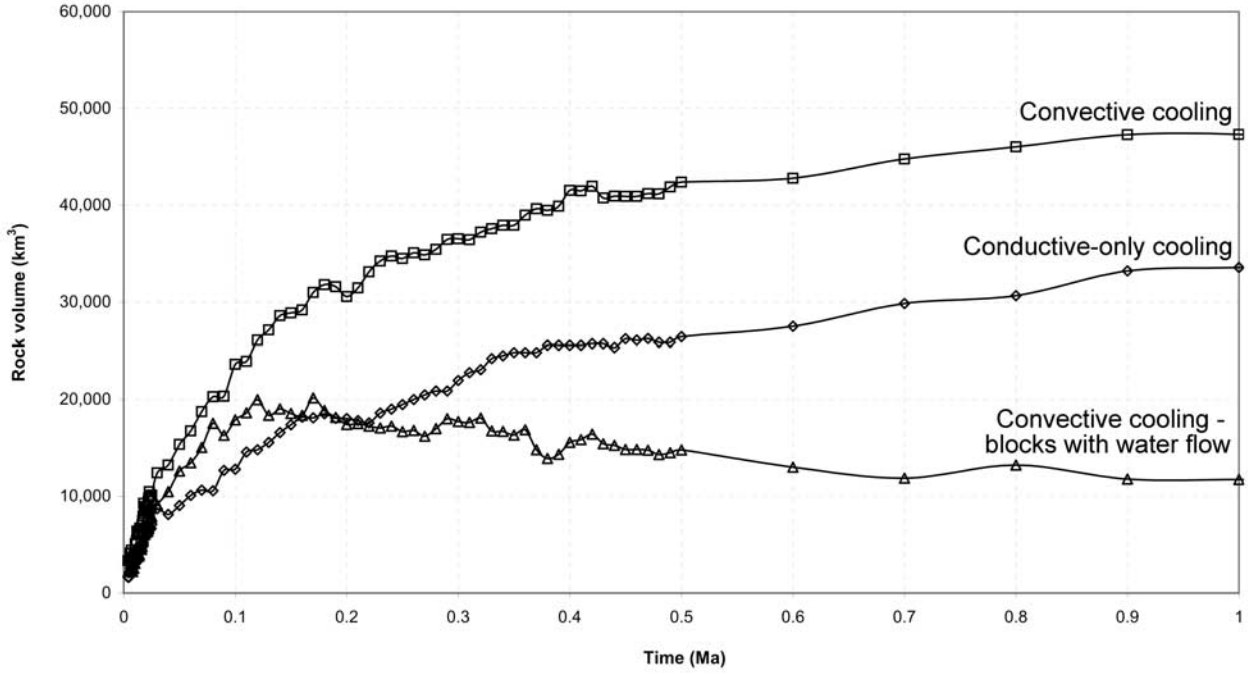

Figure 8. Rock volume between 50°C and 100°C within the crater bowl. The preimpact rock volume within this temperature range is ~50,000 km^3. "Water flow" through a block is defined as a flux of more than 1% of the maximum flux found in the system throughout its lifetime. The surface permeability, k_0, is 10^{-2} darcies.

of the breccia overburden) show evidence of widespread silicification and Ca-Na ion exchange (albitization) [*Ames et al.*, 1998]. In our model, the hydrothermal temperatures in these alteration zones reach a maximum of 300°C–400°C, which corresponds well with the observed mineral assemblages. Meanwhile, rocks of the upper Onaping formation, which is the upper 1000 m of the breccia overburden, have undergone chloritization, calcitization, and feldspathization [*Ames et al.*, 1998], which are generally associated with lower temperatures. Our model indicates that hydrothermal temperatures in most of the upper Onaping formation did not exceed 300°C, which again corresponds well with the mineralogical data.

[46] Another noteworthy feature seen in our simulations is the upwelling of water in the region along the outer wall of the crater. In large terrestrial impact craters this region contains numerous extensional faults caused by the postimpact slumping of the crater wall, which can serve as conduits for water flow. The venting of water and steam through these faults has been observed at the 24 km Haughton crater in the arctic Canada and is described by *Osinski et al.* [2001].

[47] One of the primary motivations for the study of impact-induced hydrothermal systems is the evaluation of their ability to support a long-lived ecosystem. Of particular interest is the temperature range of 50°C to 100°C, which represents a habitable zone for thermophilic organisms commonly found in hydrothermal systems. The evolution of rock volume in this temperature range within the crater bowl is shown in Figure 8. Initially after the impact, the environment within the crater bowl is too hot for thermophilic organisms to flourish, but at the same time, temperatures are increased in the periphery of the crater, creating a large rock volume between 50°C and 100°C. There is, however, little water flow through that volume after the initial draining of the rim. As the interior of the crater bowl cools, the volume of rock within the temperature range of interest increases. When the circulating water is present the crater bowl cools quicker, and the rock volume within the thermophile habitable zone increases faster. Perhaps of greater interest is the volume of rock between 50°C and 100°C that has water flow through it, defined here as more than 1% of the maximum flux seen in the system throughout its lifetime. This represents an active hydrothermal environment, which reaches a maximum volume of 20,170 km^3 at 0.17 Ma for the k_0 of 10^{-2} darcies. The total rock volume at 50°C to 100°C before the impact was ~50,000 km^3, but that volume was several kilometers below the surface and had essentially no water flow through it.

[48] An important property of long-lived hydrothermal systems not modeled in this paper is the decrease of permeability and porosity over time due to the deposition of hydrothermal minerals in the rock matrix. This effect been observed at terrestrial hydrothermal systems such as the one at Yellowstone, Wyoming [e.g., *Dobson et al.*, 2003] and in some instances can lead to a total self-sealing of the system. The mechanism for this is not well understood and can depend significantly on the mineralogy of the host rock. One possible way of constraining the importance of this parameter in the future is through the analysis of core samples from the Chicxulub Scientific Drilling Project [*Dressler et al.*, 2003], which can shed light on the relationship between flow duration (and thus hydrothermal

alteration) and permeability in an impact-induced hydrothermal system.

6. Conclusions

[49] Numerical modeling results suggest the evolution of a postimpact hydrothermal system at the Sudbury crater proceeded as follows. The first step was gravity-driven rapid draining of the rim and the flooding of the crater cavity. The water fluxes seen at this stage were generally an order of magnitude greater than those encountered in the later stages of the hydrothermal system. The interaction between the incoming water and the hot interior of the crater would have produced large quantities of steam, although we did not model the detailed venting of this steam. Eventually, a crater lake should have formed in the bowl of the crater, changing the flow of water from a gravity-driven to a hot spot–driven state. Over time, long-lived upwellings would have developed, most notably at the site of the crystallized small melt sheet and at the peak ring. Because the boiling point of water increases rapidly with pressure, steam production was probably limited to near-surface regions, except for production of supercritical fluid deep below the surface. Therefore once the near-surface cooled there was probably no steam emission from the ground in that region. The crater was cooling from the outside inward, because of a centrally located melt sheet (Sudbury Igneous Complex) and central uplift heat sources. The volume of rock between 50°C and 100°C, which represented a possible habitable zone for thermophilic organisms, increased over the lifetime of the crater. However, the rock volume in this temperature range that has water flowing through it reached a maximum at 170,000 years.

[50] In more general terms, the simulations presented in this paper show that a hydrothermal system at a large impact crater can remain active from several hundred thousand to several millions of years, depending on permeability. These long lifetimes are partly explained by the most vigorous circulation taking place near the surface and the hotter parts of the model being impermeable because of the brittle/ductile transition at about 360°C. Thus conduction remains the dominant form of heat transport in much of the model. Another important consideration is the vertical heat transport by flowing water, which can increase the temperature of near-surface regions and prolong the lifetime of the system. The results allow for long-lived near-surface ecosystems of thermophiles to be established when an impact event increases temperatures near the surface and provides a heat source to drive the circulating water. Overall, the simulations suggest that an impact-induced hydrothermal system can remain active for sufficiently long periods of time to be biologically significant, supporting the idea that impact events may have played an important biological role, especially early in Earth's history. Thus impact cratering may be creating new habitats, while at the same time destroying others.

[51] **Acknowledgments.** This work was supported by a subcontract from Arizona State University to the University of Arizona through NASA's Astrobiology Program and NASA grant NAG512691 from the Mars Fundamental Research Program. We thank Doreen Ames and Stephen Prevec for their constructive and thorough reviews of this manuscript. We also thank Lukas Zürcher and James Richardson for several helpful discussions and comments.

References

Allen, C. C., J. L. Gooding, and K. Keil (1982), Hydrothermally altered impact melt rock and breccia: Contributions to the soil of Mars, *J. Geophys. Res.*, *87*, 10,083–10,101.

Ames, D. E., and H. L. Gibson (1995), Controls on and geological setting of regional hydrothermal alteration within the Onaping Formation, footwall to the Errington and Vermilion base metal deposits, Sudbury structure, Ontario, *Pap. Geol. Survey Can.*, *1995-E*, 161–173.

Ames, D. E., H. L. Gibson, and I. R. Jonasson (1997), Impact-induced hydrothermal base metal mineralization, Whitewater group, Sudbury structure, paper presented at Large Meteorite Impacts and Planetary Evolution, Lunar and Planet. Inst., Sudbury, Ont., Canada.

Ames, D. E., D. H. Watkinson, and R. R. Parrish (1998), Dating of a regional hydrothermal system induced by the 1850 Ma Sudbury impact event, *Geology*, *26*, 447–450.

Ames, D. E., J. P. Golightly, P. C. Lightfoot, and H. L. Gibson (2002), Vitric compositions in the Onaping Formation and their relationship to the Sudbury Igneous Complex, Sudbury structure, *Econ. Geol.*, *97*, 1541–1562.

Ariskin, A. A., A. Deutsch, and M. Ostermann (1999), The Sudbury "Igneous" Complex: Simulating phase equilibria and in situ differentiation for two proposed parental magmas, in *Large Meteorite Impacts and Planetary Evolution II*, edited by B. O. Dressler and V. L. Sharpton, *Spec. Pap. Geol. Soc. Am.*, *339*, 337–387.

Binder, A. B., and M. A. Lange (1980), On the thermal history, thermal state, and related tectonism of a moon of fission origin, *J. Geophys. Res.*, *85*, 3194–3208.

Brace, W. F. (1980), Permeability of crystalline and argillaceous rocks, *Int. J. Rock Mech. Min. Sci. Geomech. Abstr.*, *17*, 241–251.

Brace, W. F. (1984), Permeability of crystalline rocks: New measurements, *J. Geophys. Res.*, *89*, 4327–4330.

Brockmeyer, P. (1990), Petrographie, Geochemie und Isotopenuntersuchungen an der Onaping-Formation im Nordteil der Sudbury-Struktur (Ontario, Kanada) und ein Modell zur Genese der Struktur, dissertation, 228 pp., Inst. für Planetol., Univ. Münster, Münster, Germany.

Clifford, M. (1993), A model for the hydrologic and climatic behavior of water on Mars, *J. Geophys. Res.*, *98*, 10,973–11,016.

Cohen, B. A., T. D. Swindle, and D. A. Kring (2000), Support for the lunar cataclysm hypothesis from lunar meteorite impact melt ages, *Science*, *290*, 1754–1756.

Collins, G. S., H. J. Melosh, J. V. Morgan, and M. R. Warner (2002), Hydrocode simulations of Chicxulub crater collapse and peak-ring formation, *Icarus*, *157*, 24–33.

Daubar, I. J., and D. A. Kring (2001), Impact-induced hydrothermal systems: Heat sources and lifetimes, *Lunar Planet. Sci.* [CD-ROM], *XXXII*, Abstract 1727.

Dobson, P. F., T. J. Kneafsey, J. Hulen, and A. Simmons (2003), Porosity, permeability, and fluid flow in the Yellowstone geothermal system, Wyoming, *J. Volcanol. Geotherm. Res.*, *123*, 313–324.

Donnelly-Nolan, J. M., M. G. Burns, F. E. Goff, E. K. Peters, and J. M. Thompson (1993), The Geysers-Clear Lake area, California: Thermal waters, mineralization, volcanism, and geothermal potential, *Econ. Geol.*, *88*, 301–316.

Dressler, B. O. (1984a), General geology of the Sudbury area, in *The Geology and Ore Deposits of the Sudbury Structure*, edited by E. G. Pye et al., pp. 57–82, Minist. of Nat. Resour., Toronto, Ont., Canada.

Dressler, B. O. (1984b), The effects of the Sudbury event and the intrusion of the Sudbury igneous complex on the footwall rocks of the Sudbury structure, in *The Geology and Ore Deposits of the Sudbury Structure*, edited by E. G. Pye et al., pp. 97–136, Minist. of Nat. Resour., Toronto, Ont., Canada.

Dressler, B. O., W. V. Peredery, and T. L. Muir (1992), Geology and mineral deposits of the Sudbury structure, in *Ontario Geological Survey Guidebook 8*, report, 38 pp., Minist. of North. Dev. and Mines, Toronto, Ont., Canada.

Dressler, B. O., T. Weiser, and P. Brockmeyer (1996), Recrystallized impact glasses of the Onaping Formation and the Sudbury Igneous Complex, Sudbury structure, Ontario, Canada, *Geochim. Cosmochim. Acta*, *60*, 2019–2036.

Dressler, B. O., V. L. Sharpton, J. Morgan, R. Buffler, D. Moran, J. Smit, D. Stöffler, and J. Urrutia (2003), Investigating a 65-Ma-old smoking gun: Deep drilling of the Chicxulub impact structure, *Eos Trans. AGU*, *84*(14), 125–130.

Farrow, C. E. G., and D. H. Watkinson (1992), Alteration and the role of fluids in Ni, Cu and platinum-group element deposition, Sudbury Igneous Complex contact, Onaping-Levack area, Ontario, *Mineral. Petrol.*, *46*, 611–619.

Farrow, C. E. G., and D. H. Watkinson (1997), Diversity of precious-metal mineralization in the footwall Cu-Ni-PGE deposits, Sudbury, Ontario: Implications for hydrothermal models of formation, *Can. Mineral.*, *35*, 817–839.

Faust, C. R., and J. W. Mercer (1977), A finite-difference model of two-dimensional, single- and two-phase heat transport in a porous medium-version I, *U.S. Geol. Surv. Open File Rep.*, *77-234*, 47 pp.

Faust, C. R., and J. W. Mercer (1979a), Geothermal reservoir simulation: 1. Mathematical models for liquid and vapor-dominated hydrothermal systems, *Water Resour. Res.*, *15*(1), 23–30.

Faust, C. R., and J. W. Mercer (1979b), Geothermal reservoir simulation: 2. Numerical solution techniques for liquid and vapor-dominated hydrothermal systems, *Water Resour. Res.*, *15*(1), 31–46.

Fournier, R. O. (1989), Geochemistry and dynamics of the Yellowstone National Park hydrothermal system, *Annu. Rev. Earth Planet. Sci.*, *17*, 13–53.

Fournier, R. O. (1991), The transition from hydrostatic to greater than hydrostatic fluid pressure in presently active continental hydrothermal systems in crystalline rock, *Geophys. Res. Lett.*, *18*, 955–958.

French, B. M. (1967), Sudbury structure, Ontario: Some petrographic evidence for an origin by meteorite impact, *Science*, *156*, 1094–1098.

French, B. M. (1968), Sudbury structure, Ontario: Some petrographic evidence for an origin by meteorite impact, in *Shock Metamorphism of Natural Materials*, edited by B. M. French and N. M. Short, pp. 383–412, Mono Book, Baltimore, Md.

Ganguly, J., R. N. Singh, and D. V. Ramana (1995), Thermal perturbation during charnockitization and granulite facies metamorphism in southern India, *J. Metamorph. Geol.*, *13*, 419–430.

Garvin, J. B., S. E. H. Sakimoto, J. J. Frawley, and C. Schnetzler (2002), Global geometric properties of Martian impact craters, *Lunar Planet. Sci.* [CD-ROM], *XXXIII*, Abstract 1255.

Giblin, P. E. (1984), History of exploration and development, of geological studies and development of geological concepts, in *The Geology and Ore Deposits of the Sudbury Structure*, edited by E. G. Pye et al., pp. 3–23, Minist. of Nat. Resour., Toronto, Ont., Canada.

Grieve, R. A. F. (1994), An impact model of the Sudbury structure, in *Proceedings of the Sudbury-Noril'sk Symposium*, edited by P. C. Lightfoot and A. J. Naldrett, Ont. Geol. Surv. Spec. Vol., 5, 119–132.

Grieve, R. A. F., and M. J. Cintala (1992), An analysis of differential impact melt-crater scaling and implications for the terrestrial impact record, *Meteoritics*, *27*, 526–538.

Grieve, R. A. F., D. Stöffler, and A. Deutsch (1991), The Sudbury structure: Controversial or misunderstood?, *J. Geophys. Res.*, *96*, 22,753–22,764.

Grieve, R. A. F., J. Rupert, J. Smith, and A. Therriault (1995), The record of terrestrial impact cratering, *GSA Today*, *5*(189), 194–196.

Hale, W., and R. A. F. Grieve (1982), Volumetric analysis of complex lunar craters: Implications for basin ring formation, *J. Geophys. Res.*, *87*, A65–A76, suppl.

Hanson, R. B. (1995), The hydrodynamics of contact metamorphism, *Geol. Soc. Am. Bull.*, *107*(5), 595–611.

Hayba, D. O., and S. E. Ingebritsen (1994), The computer model HYDROTHERM, a three-dimensional finite-difference model to simulate ground-water flow and heat transport in the temperature range of 0 to 1,200°C, *U.S. Geol. Surv. Water Resour. Invest. Rep., 94-4045*, 85 pp.

Hayba, D. O., and S. E. Ingebritsen (1997), Multiphase groundwater flow near cooling plutons, *J. Geophys. Res.*, *102*, 12,235–12,252.

Henry, C. D., H. B. Elson, W. C. McIntosh, M. T. Heizler, and S. B. Castor (1997), Brief duration of hydrothermal activity at Round Mountain, Nevada determined from $^{40}Ar/^{39}Ar$ geochronology, *Econ. Geol.*, *92*, 807–826.

Hildebrand, A. R., M. Pilkington, C. Ortiz-Aleman, R. E. Chavez, J. Urrutia-Fucugauchi, M. Connors, E. Graniel-Castro, A. Camara-Zi, J. A. Halpenny, and D. Niehaus (1998), Mapping Chicxulub crater structure with gravity and seismic reflection data, in *Meteorites: Flux With Time and Impact Effects*, edited by M. M. Grady et al., *Geol. Soc, Spec. Publ.*, *140*, 153–173.

Ivanov, B. A., and A. Deutsch (1999), Sudbury impact event: Cratering mechanics and thermal history, in *Large Meteorite Impacts and Planetary Evolution II*, edited by B. O. Dressler and V. L. Sharpton, *Spec. Pap. Geol. Soc. Am.*, *339*, 389–397.

Jaeger, J. C. (1968), Cooling and solidification of igneous rocks in basalts, in *The Poldervaart Treatise on Rocks of Basaltic Composition*, edited by H. H. Hess and A. Poldervaart, pp. 503–535, John Wiley, Hoboken, N. J.

Kahle, H. G. (1969), Abschätzung der Störungsmasse im Nördlinger Ries, *Z. Geophys.*, *35*, 317–345.

Kring, D. A. (2000), Impact events and their effect on the origin, evolution, and distribution of life, *GSA Today*, *10*, 1–7.

Kring, D. A., and W. V. Boynton (1992), Petrogenesis of an augite-bearing melt rock in the Chicxulub structure and its relationship to K/T impact spherules in Haiti, *Nature*, *358*, 141–144.

Kring, D. A., and B. A. Cohen (2002), Cataclysmic bombardment throughout the inner solar system 3.9–4. 0 Ga, *J. Geophys. Res.*, *107*(E2), 5009, doi:10.1029/2001JE001529.

Krogh, T. E., D. W. Davis, and F. Corfu (1984), Precise U-Pb zircon and baddeleyite ages for the Sudbury area, in *The Geology and Ore Deposits of the Sudbury Structure*, edited by E. G. Pye et al., pp. 431–446, Minist. of Nat. Resour., Toronto, Ont., Canada.

Lakomy, R. (1990), Implications of cratering mechanics from a study of the footwall breccia of the Sudbury impact structure, Canada, *Meteoritics*, *25*, 195–207.

McCarville, P., and L. J. Crossey (1996), Post-impact hydrothermal alteration of the Manson impact structure, Manson, Iowa, in *The Manson Impact Structure, Iowa: Anatomy of an Impact Crater*, edited by C. Koeberl and R. R. Anderson, *Spec. Pap. Geol. Soc. Am.*, *302*, 347–376.

Melosh, H. J. (1989), *Impact Cratering: A Geologic Process*, 245 pp., Oxford Univ. Press, New York.

Milkereit, B., and A. Green (1992), Deep geometry of the Sudbury structure from seismic reflection profiling, *Geology*, *20*, 807–811.

Mojzsis, S. J., and T. M. Harrison (2000), Vestiges of a beginning: Clues to the emergent biosphere recorded in the oldest known sedimentary rocks, *GSA Today*, *10*, 1–6.

Molnár, F., D. H. Watkinson, P. C. Jones, and I. Gatter (1999), Fluid inclusion evidence for hydrothermal enrichment of magmatic ores at the contact zone of the Ni-Cu-platinum group element, 4b Deposit, Lindsley Mine, Sudbury, Canada, *Econ. Geol.*, *92*, 674–685.

Morgan, J., M. Warner, and the Chicxulub Working Group (1997), Size and morphology of the Chicxulub impact crater, *Nature*, *390*, 472–476.

Muir, T. L., and W. V. Peredery (1984), The Onaping Formation, in *The Geology and Ore Deposits of the Sudbury Structure*, edited by E. G. Pye et al., pp. 139–210, Minist. of Nat. Resour., Toronto, Ont., Canada.

Naldrett, A. J., R. H. Hewins, B. O. Dressler, and B. V. Rao (1984), The contact sublayer of the Sudbury igneous complex, in *The Geology and Ore Deposits of the Sudbury Structure*, edited by E. G. Pye et al., pp. 253–274, Minist. of Nat. Resour., Toronto, Ont., Canada.

Naumov, M. V. (1993), Zonation of hydrothermal alteration in the central uplift of the Puchezh-Katunki astrobleme, *Meteoritics*, *28*, 408–409.

Naumov, M. V. (2002), Impact-generated hydrothermal systems: Data from Popigai Kara, and Puchezh-Katunki impact structures, in *Impacts in Precambrian Shields*, edited by J. Plado and L. J. Pesonen, pp. 117–171, Springer-Verlag, New York.

Newsom, H. E. (1980), Hydrothermal alteration of impact melt sheets with implications for Mars, *Icarus*, *44*, 207–216.

Newsom, H. E., G. E. Brittelle, C. A. Hibbitts, L. J. Crossey, and A. M. Kudo (1996), Impact crater lakes on Mars, *J. Geophys. Res.*, *101*, 14,951–14,956.

Onorato, P. I. K., D. R. Uhlmann, and C. H. Simonds (1978), The thermal history of the Manicouagan impact melt sheet, Quebec, *J. Geophys. Res.*, *83*, 2789–2798.

Osinski, G. R., J. G. Spray, and P. Lee (2001), Impact-induced hydrothermal activity in the Haughton impact structure, Canada: Generation of a transient, warm, wet oasis, *Meteorit. Planet. Sci.*, *36*, 731–745.

Pace, N. R. (1997), A molecular view of microbial diversity and the biosphere, *Science*, *276*, 734–740.

Peredery, W. V. (1972), Chemistry of fluidal glasses and melt bodies in the Onaping Formation, in *New Developments in Sudbury Geology*, edited by J. V. Guy-Bray, *Geol. Assoc. Can. Spec. Pap.*, *10*, 49–59.

Peredery, W. V., and G. G. Morrison (1984), Discussion of the origin of the Sudbury structure, in *The Geology and Ore Deposits of the Sudbury Structure*, edited by E. G. Pye et al., pp. 491–511, Minist. of Nat. Resour., Toronto, Ont., Canada.

Pike, R. (1977), Size dependence in the shape of fresh impact craters on the Moon, in *Impact and Explosion Cratering*, edited by D. J. Roddy et al., pp. 489–509, Pergamon, New York.

Pike, R. (1985), Some morphologic systematics of complex impact structures, *Meteoritics*, *20*, 49–68.

Press, W. H., B. P. Flannery, S. A. Teukolsky, and W. T. Vetterling (1986), *Numerical Recipes: The Art of Scientific Computing*, Cambridge Univ. Press, New York.

Prevec, S. A., and R. G. Cawthorn (2002), Thermal evolution and interaction between impact melt sheet and footwall: A genetic model for the contact sublayer of the Sudbury Igneous Complex, Canada, *J. Geophys. Res.*, *107*(B8), 2176, doi:10.1029/2001JB000525.

Prevec, S. A., P. C. Lightfoot, and R. R. Keays (2000), Evolution of the sublayer of the Sudbury Igneous Complex: Geochemical, Sm-Nd isotopic and petrologic evidence, *Lithos*, *51*, 271–292.

Pye, E. G., A. J. Naldrett, and P. E. Giblin (Eds.) (1984), *The Geology and Ore Deposits of the Sudbury Structure*, 604 pp., Minist. of Nat. Resour., Toronto, Ont., Canada.

Rathbun, J. A., and S. W. Squires (2002), Hydrothermal systems associated with Martian impact craters, *Icarus*, *157*, 362–372.

Rousell, D. H. (1984a), Structural geology of the Sudbury basin, in *The Geology and Ore Deposits of the Sudbury Structure*, edited by E. G. Pye et al., pp. 83–95, Minist. of Nat. Resour., Toronto, Ont., Canada.

Rousell, D. H. (1984b), Onwatin and Chelmsford formations, in *The Geology and Ore Deposits of the Sudbury Structure*, edited by E. G. Pye et al., pp. 211–218, Minist. of Nat. Resour., Toronto, Ont., Canada.

Rousell, D. H. (1984c), Mineralization in the Whitewater group, in *The Geology and Ore Deposits of the Sudbury Structure*, edited by E. G. Pye et al., pp. 219–232, Minist. of Nat. Resour., Toronto, Ont., Canada.

Ryder, G. (1990), Lunar samples, lunar accretion and the early bombardment of the Moon, *Eos Trans. AGU*, *71*(10), 313, 322–323.

Sclater, J. G., C. Jaupart, and D. Galson (1980), The heat flow through oceanic and continental crust and the heat loss of the earth, *Rev. Geophys.*, *18*, 269–311.

Tera, F., D. A. Papanastassiou, and G. J. Wasserburg (1974), Isotopic evidence for a terminal lunar cataclysm, *Earth Planet. Sci. Lett.*, *22*, 1–21.

Therriault, A. M., A. D. Fowler, and R. A. F. Grieve (2002), The Sudbury Igneous Complex: A differentiated impact melt, *Econ. Geol.*, *97*, 1521–1540.

Travis, B. J., D. R. Janecky, and N. D. Rosenberg (1991), Three-dimensional simulation of hydrothermal circulation at mid-ocean ridges, *Geophys. Res. Lett.*, *18*(8), 1441–1444.

Turner, G., P. H. Cadogan, and C. J. Yonge (1973), Argon selenochronology, *Proc. Lunar Sci. Conf.*, *IV*, 1889–1914.

Turtle, E. P., E. Pierazzo, and D. P. O'Brien (2003), Numerical modeling of impact heating of the Vredefort impact structure, *Meteorit. Planet. Sci.*, *38*, 293–303.

Warnaars, F. W., W. H. Smith, R. E. Bray, G. Lanier, and M. Shafiqullah (1978), Geochronology of igneous intrusions and porphyry copper mineralization at Bingham, Utah, *Econ. Geol.*, *73*, 1242–1249.

Warren, P. H., and K. L. Rasmussen (1987), Megaregolith insulation, internal temperatures, and the bulk uranium content of the moon, *J. Geophys. Res.*, *92*, 3453–3465.

Wichman, R. W., and P. H. Schultz (1993), Floor-fractured crater models of the Sudbury structure, Canada: Implications for initial crater size and crater modification, *Meteoritics*, *28*, 222–231.

Wood, C. A., and J. W. Head (1976), Comparison of impact basins on Mercury, Mars, and the Moon, *Proc. Lunar Sci. Conf.*, *VII*, 3629–3651.

Wu, J., B. Milkereit, and D. Boerner (1994), Timing constraints on deformation history of the Sudbury impact structure, *Can. J. Earth Sci.*, *31*, 1654–1660.

Wu, J., B. Milkereit, and D. E. Boerner (1995), Seismic imaging of the enigmatic Sudbury structure, *J. Geophys. Res.*, *100*, 4117–4130.

Zahnle, K. J., and N. H. Sleep (1997), Impacts and the early evolution of life, in *Comets and the Origin and Evolution of Life*, edited by P. J. Thomas et al., pp. 175–208, Springer-Verlag, New York.

Zürcher, L., and D. A. Kring (2004), Hydrothermal alteration in the Yaxcopoil-1 borehole, Chicxulub impact structure, Mexico, *Meteorol. Planet. Sci.*, *39*(7), 1199–1222.

O. Abramov and D. A. Kring, Lunar and Planetary Laboratory, University of Arizona, 1629 East University Blvd., Tucson, AZ 85721-0092, USA. (abramovo@lpl.arizona.edu)